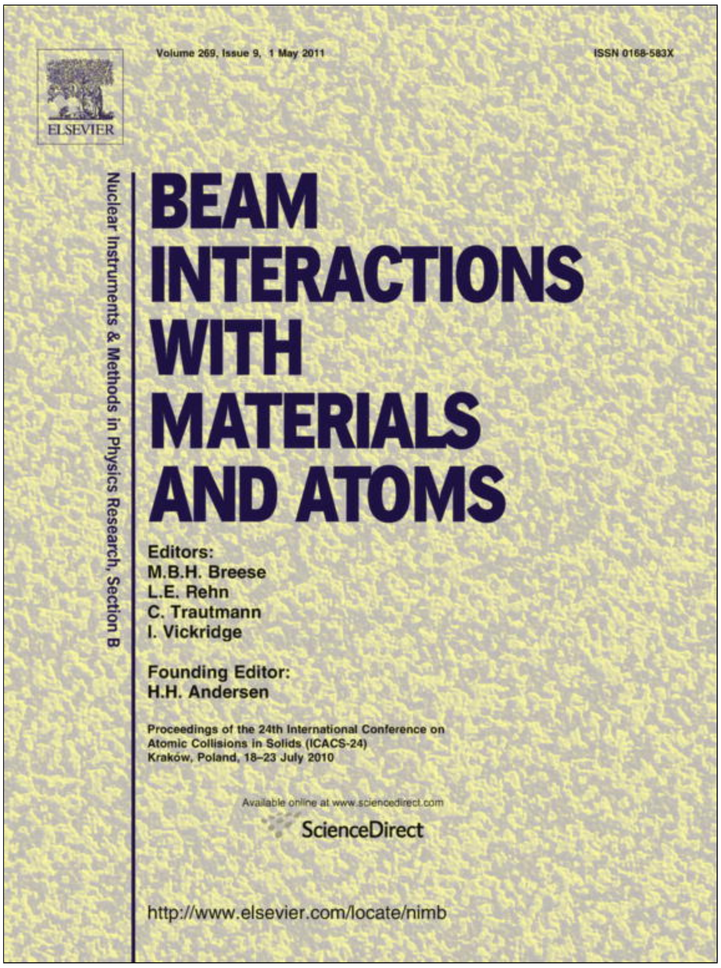

Volume 269, Issue 9, 1 May 2011
ISSN 0168-583X

ELSEVIER

Nuclear Instruments & Methods in Physics Research, Section B

BEAM
INTERACTIONS
WITH
MATERIALS
AND ATOMS

Proceedings of the 24th International Conference on
Atomic Collisions in Solids (ICACS-24)
Kraków, Poland, 18–23 July 2010

Nuclear Instruments and Methods in Physics Research B 269 (2011) 915–918

Contents lists available at ScienceDirect

Nuclear Instruments and Methods in Physics Research B

journal homepage: www.elsevier.com/locate/nimb

Negative ion formation during scattering of fast ions from diamond-like carbon surfaces

J. Lienemann [a], D. Blauth [a], S. Wethekam [a], M. Busch [a,*], H. Winter [a], P. Wurz [b], S.A. Fuselier [c], E. Hertzberg [c]

[a] *Institut für Physik der Humboldt-Universität zu Berlin, Newtonstrasse 15, D-12489 Berlin-Adlershof, Germany*
[b] *Physikalisches Institut, Universität Bern, Sidlerstrasse 5, CH-3012 Bern, Switzerland*
[c] *Lockheed Martin Advanced Technology Center, 3251 Hanover Street, Palo Alto, CA, USA*

ARTICLE INFO

Article history:
Received 29 July 2010
Received in revised form 9 November 2010
Available online 26 November 2010

ABSTRACT

Fractions of negative ions after grazing scattering of fast hydrogen and oxygen atoms and ions from diamond-like carbon (DLC) surfaces are studied as function of projectile velocity. We reveal a pronounced kinematic resonance behaviour for the negative ion fractions as function of projectile velocity which provides important information on the charge transfer mechanism. The conversion of neutral atoms into negative ions during scattering from DLC surfaces is used for the detection of energetic neutral atoms in space.

1. Introduction

Scattering of fast atoms and ions from solid surfaces is accompanied by charge exchange which plays an important role in a variety of applications such as discharge phenomena, surface analytical tools, plasma-wall interactions, and particle detection. In the latter application, one finds interesting recent applications in the detection of energetic neutral atoms (ENA), i.e., atoms with kinetic energies from 10 eV to 1 MeV, for remote sensing of space plasma populations [1]. Here the detection of ENA is used to study the various plasma entities of the terrestrial magnetosphere, the magnetospheres of other planets, and even the plasma surrounding our solar system beyond the heliospheric termination shock [2]. Remote sensing via ENA detection marked a major improvement over the *in situ* space plasma measurements with ion detection instruments [3,4].

With an instrument, which not only records the mass and the energy of ENA but also records the arrival direction in one or two dimensions, 2D maps of such plasma distributions are obtained, which are line-of-sight integrals of 3D plasma distributions [3]. A particularly difficult energy range for ENA detection is for energies ranging from 10 eV to a few keV [5]. In view of the limitations in available mass and power, as well as the limited complexity of an autonomously operating instrument on a space platform, surface ionization is presently a feasible technique that can be used in this energy range, where negative ions are formed during scattering from a suitable surface [3]. In recent years, a variety of different surfaces and surface coatings have been investigated for this application, requiring low angular and energy spread as well as sufficient negative ion yields for the reflected beam. It turned out that diamond targets showed attractive features for ENA detection, because those can be prepared with a flat surface and are chemically inert [6]. The latter aspect is important for space flight missions, since an instrument cannot be kept in good vacuum or in a controlled atmosphere during launch. Since natural diamonds are costly, amorphous carbon (a-C) coatings on silicon wafers were used which satisfy most requirements for space applications. These surface coatings can be produced in good quality and in large quantities [4].

Despite successful operation of instruments equipped with DLC targets, the mechanism for charge exchange, in particular the formation of negative ions is so far not understood. The work presented here is a detailed study of kinematic features of the formation of negative ions during scattering from DLD surfaces. Whereas the range of projectile velocities was fairly limited in previous studies, we performed experiments over a much wider range in order to obtain information on the microscopic interaction mechanisms.

2. Experiment and results

We measured fractions of negative ions for scattering of hydrogen and oxygen atoms/ions from the surface of a tetrahedral amorphous carbon coating on a silicon wafer. This type of surface was used in previous studies and in a space mission [1]. The experiments were performed in an ultra high vacuum (UHV) chamber at a base pressure in the 10^{-10} mbar range. H^+ and O^+ ions were produced in an Electron Cyclotron Resonance (ECR) ion source operated at a microwave frequency of 14.5 GHz and neutralized in a gas target. The energy of the fast atoms and positive ions was varied over a wide range of projectile energies

---

* Corresponding author.
E-mail address: mbusch@physik.hu-berlin.de (M. Busch).

0168-583X/$ - see front matter © 2010 Elsevier B.V. All rights reserved.
doi:10.1016/j.nimb.2010.11.054

between about 100 eV and 300 keV. This considerably larger range of energies compared to previous studies allows us to investigate kinematic features of negative ion formation in details, i.e., to study complete kinematic resonances for the negative ion fractions [7–13].

The DLC surface was a tetrahedral amorphous carbon (ta-C) film about 1000 Å thick deposited on a Si wafer [3] and was mounted on a precision manipulator. We checked by means of Auger Electron Spectroscopy (AES) that after preparation of the target by heating to about 600 °C and grazing sputtering with 50 keV Ar^+ ions the surface was free from impurities as, e.g., species containing oxygen atoms. The well-collimated beam of neutral atoms (divergence abpit 1 mrad = 0.057 deg) was directed at a grazing angle of incidence between $\Phi_{in} = 1$ deg and $\Phi_{in} = 2$ deg onto the DLC surface. Since the surface roughness of the samples used here was a few Å, the beam of scattered projectiles was broadened compared to experiments with atomically flat surfaces of mono-crystalline samples.

Angular distributions of scattered beams were recorded by means of a 2D position sensitive micro-channel plate (MCP) detector [14] where individual positions of impinging fast atoms/ions on the active detector surface were obtained via a delay line anode. This detector was mounted 0.7 m behind the target and typical count rates amounted to some 1000 counts per second. As an example we show in Fig. 1 the (projected) polar angular distribution for 20 keV He^+ ions scattered from a DLC target under a grazing angle of incidence of $\Phi_{in} = 1.3$ deg showing a defined peak structure with a full width at half maximum (FWHM) of 2.1 deg. Angular distributions recorded for grazing ion surface collisions are very sensitive to the defect structure of the target surface and can be analyzed in this respect [15,16]. Compared to scattering from well-defined surfaces of mono-crystalline samples with terrace widths of some 100 Å, the distribution shown in Fig. 1 is clearly broader and reflects the roughness of a polycrystalline sample. The procedure for the preparation of clean and flat crystal surfaces, i.e., grazing sputtering with Ar^+ ions of some 10 keV and subsequent annealing up to 600 °C, was not successful to improve the angular distributions and the "quality" of the target. On the other hand, a scattered beam with an angular distribution as shown in Fig. 1 is still sufficiently well defined for studies on charge transfer and for applications.

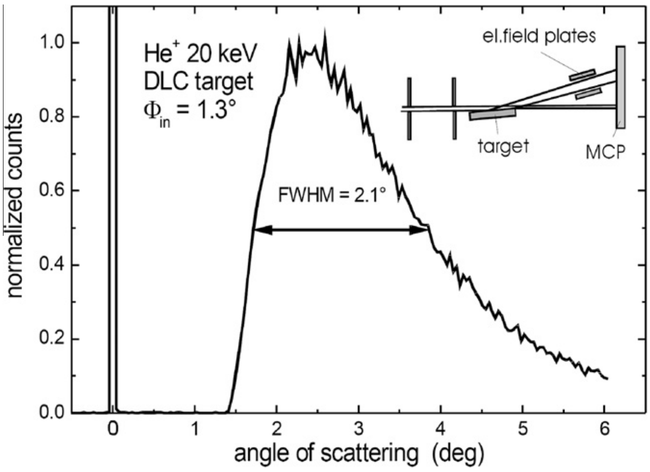

Fig. 1. Polar angular distribution for scattering of 20 keV He^+ ions from DLC surface under $\Phi_{in} = 1.3$ deg recorded with position sensitive MCP detector (projection onto polar angle). Intense peak at left side stems from residual portion of beam passing target without interaction and defines zero of scale for polar angle. A sketch of scattering geometry and essential parts of setup is given in inset.

Charge fractions were obtained by dispersing the scattered particles of different charge in a transverse electric field between target and detector. In Fig. 2 we show charge fractions for scattering of H^+ ions from a DLC surface under $\Phi_{in} = 1.0$ deg (full circles) and $\Phi_{in} = 1.5$ deg (full squares) as function of projectile velocity. The upper panel displays the neutral fractions which dominate the charge state spectrum within the range of projectile velocities studied here ($v < 1$ a.u. $= v_o =$ Bohr velocity). At low velocities the scattered beam is fully neutralized, and with increasing velocity the neutral fractions decrease to about 80% at $v = 0.9$ a.u. In the lower panel we display negative (full symbols) and positive (crosses) ion fractions. The negative ion fractions show a kinematic resonance with a maximum of about 5% at about $v = 0.35$ a.u. Whereas the onset part for the negative ion fractions below the maximum was observed already in previous studies and shows similar values as in former work [17], the resonance structure is observed herein for the first time. We will discuss below that how this feature provides an important input for the interpretation of data in terms of the underlying physics of the interaction mechanisms. The positive ion fractions are about a factor of three smaller for the lowest velocities of our study (~0.1 a.u.) and show a monotonic increase with velocity. At a projectile velocity of about 0.4 a.u. (energy of about 4 keV) negative and positive ions fractions

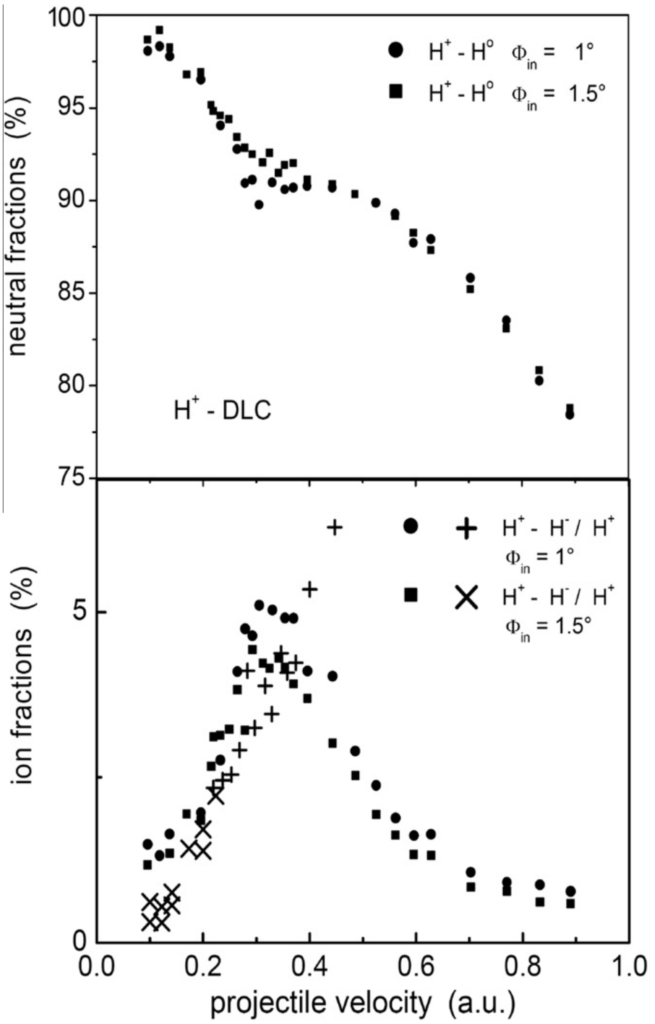

Fig. 2. Neutral (upper panel) and ion fractions (lower panel) as function of projectile velocity for scattering of H^+ ions from DLC surface. Negative ion fractions for scattering at $\Phi_{in} = 1.0$ deg (full circles) and $\Phi_{in} = 1.5$ deg (full squares). H^+ fractions for scattering under $\Phi_{in} = 1.0$ deg ("+") and $\Phi_{in} = 1.5$ deg ("×").

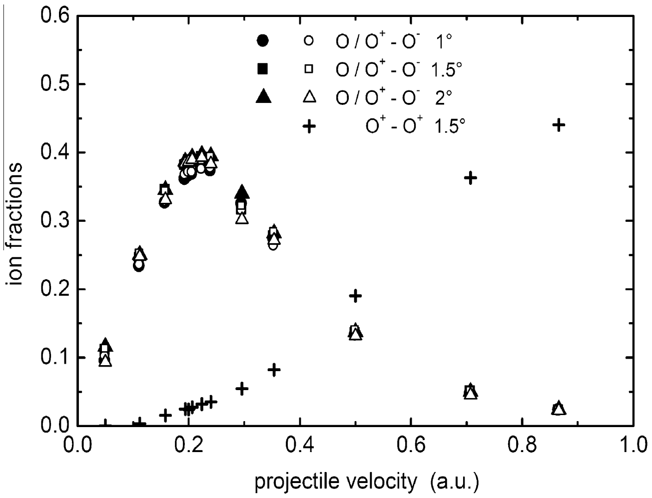

Fig. 3. Negative ion fractions as function of projectile velocity for scattering of O atoms (full symbols) and O^+ ions (open symbols) from DLC surface under $\Phi_{in} = 1.0$ deg (circles), $\Phi_{in} = 1.5$ deg (squares), and $\Phi_{in} = 2.0$ deg (triangles). Positive ion fractions for scattering at $\Phi_{in} = 1.5$ deg ("+") are shown also.

are the same. For velocities $v > 0.4$ a.u. the positive ion fractions exceed the scale of the figure.

In Fig. 3 we show negative ion fractions for the scattering of O^+ ions (open symbols) and neutral O atoms (full symbols) from a DLC target under $\Phi_{in} = 1.0$ deg (circles), $\Phi_{in} = 1.5$ deg (squares), and $\Phi_{in} = 2.0$ deg (triangles). The data show a similar kinematic resonance structure as observed for H, however, the negative ion fractions are substantially larger with a maximum value of 35% at a velocity of about 0.25 a.u. The crosses denote positive ion fractions for scattering of O^+ ions under $\Phi_{in} = 1.5$ deg. The data for scattering of O^+ ions and O atoms as well as of H^+ ions and H atoms (not shown) do not indicate within the accuracy of the experiment an effect on the charge of the projectiles. This observation can serve as a signature of a charge state equilibrium in the interaction process where a memory to the charge state of the incident particle is lost.

3. Discussion

For the formation of negative ions during scattering of atoms or positive ions from solid surfaces it is of primary interest to achieve a general understanding for the charge exchange mechanisms. This interest is also driven by the perspective to optimize the conversion process in applications of this concept as outlined above. In recent decades, detailed studies on the conversion of atoms/ions into negative ions during scattering from solid surfaces have been performed [12,16,18]. Here basically two different processes were identified which dominate the charge transfer process during the interaction with clean metal and insulator surfaces, primarily ionic crystals. In both cases the collision dynamics plays an important role for capture and loss of electrons between projectile and target surface.

For metal targets, resonant electron transfer has been revealed as the dominant process [18]. Since negative ions have (modified) binding energies smaller than the work function of the target surface, the capture of conduction electrons has to be dynamically assisted, giving rise to kinematic resonance structures for negative ion fractions [19]. During the scattering process, the projectile level is primarily in resonance with unoccupied conduction band states so that the resulting negative ion fractions are small, typically ranging from some permille up to some percent. For ionic crystals, negative ions are formed in local capture events from tightly bound electrons located at halide sites [20] where the considerable energy defect in the collision is reduced by the Madelung potential owing to the surrounding point charge lattice [21–23]. Negative ion fractions are significantly larger and amount to several percent for hydrogen and up to 60% for oxygen atoms scattered from LiF(0 0 1).

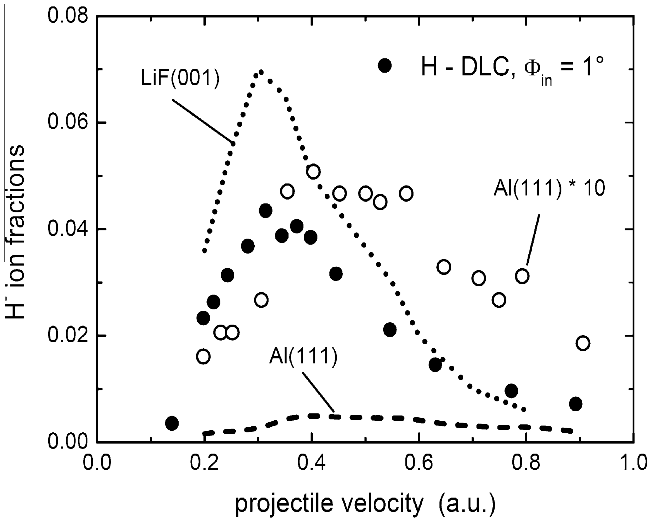

Fig. 4. Negative ion fractions as function of projectile velocity for scattering of H atoms from DLC surface under $\Phi_{in} = 1.0$ deg (full circles). Dotted curve represents data for scattering from LiF(0 0 1) [14], open circles data for Al(1 1 1) [11], thin dashed curve data for Al(1 1 1) enhanced by factor of 10.

For a more detailed comparison we have plotted in Fig. 4 negative ion fractions for the scattering of H atoms from a DLC target (solid circles) under $\Phi_{in} = 1.0$ deg and similar data obtained in former studies for scattering from an Al(1 1 1) (dashed curve) [16] and LiF(0 0 1) surface (dotted curve) [24]. The negative ion fractions for scattering from LiF(0 0 1) are slightly larger than for the DLC target, but show a similar dependence on the projectile velocity. For the metal target, however, the ion fractions are about an order of magnitude smaller and clearly reveal a resonance structure shifted to higher velocities as shown by the thin dashed curve representing the negative ion fractions for Al(1 1 1) which we enlarged by a factor of 10 in the plot. A sketch of electronic energies for the different surfaces as well as for the affinity levels of the negative hydrogen and oxygen atoms in front of the surface is given in Fig. 5. Main differences between the three targets are the energy of occupied electronic valence and conduction band states (dark grey), unoccupied conduction band states (grey), and the band gap (denoted E_G for DLC). The position of the surface

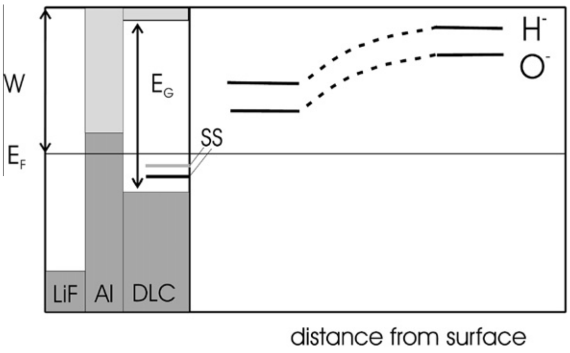

Fig. 5. Sketch of energy diagram for interaction of H^- and O^- ions with DLC, Al, and LiF surfaces. "SS" denotes surface state for different orientations of diamond surface, thin solid line position of Fermi level for diamond surface.

state (SS) depending on surface orientation is given for the DLC target.

The substantially smaller negative ion fractions for scattering from Al(1 1 1) compared to the DLC surface can be attributed to the missing band gap for the metal. During the interaction process the affinity levels of H^- and O^- are shifted via dielectric response phenomena ("image charge" interaction) to enhanced binding energies so that the energy defect to occupied metal states is reduced. This confluence of levels enhances the electron capture rates significantly. Furthermore, electron capture is kinematically assisted owing to the parallel velocity of the projectiles [16,18]. The capture process alone would favour Al compared to DLC owing to available lower binding energies of occupied electronic states. It turns out, however, that on the receding part of the trajectory the affinity levels are in resonance with unoccupied conduction band states and electron loss plays a dominant role. As a consequence, only very small negative ion fractions are observed for grazing scattering of hydrogen from clean metal surfaces [19]. For a DLC surface (and also for LiF) electron loss via resonant ionization is suppressed, because these materials have a substantial electronic band gap in the energy range for binding energies of negative ions (typically eV energies).

For negative ion formation during scattering from the surface of an ionic crystal, the Madelung potential owing to charged lattice sites is important, since this potential leads to the confluence of the affinity levels with the electronic level of active halide sites [7,21]. This effect lowers the energy defect in the collision and leads to considerable electron capture rates. Subsequent electron loss is suppressed by the broad band gap of ionic crystals and proceeds via formation of excitons and various detachment processes. Thus, despite the capture of much more tightly bound electrons than for a metal, negative ion fractions for scattering from surfaces of ionic crystals can be high and reach in specific cases almost 100% [25].

Since the H^- and O^- fractions for scattering from LiF are larger than for scattering from a DLC target, where in the latter case target electrons of lower binding energy can be captured, such local capture processes are unlikely for the diamond surface. This is consistent with the dominance of a covalent instead of an ionic bond for diamond. Therefore, we consider a mechanism of electron capture from the conduction band as for metals as a possible scenario where the electronic band gap of diamond extending from below the Fermi level close to about vacuum energies will suppress subsequent electron loss. This would result in enhanced negative ion fractions compared to a clean metal target with a high density of states for unoccupied conduction band states giving rise to substantial electron loss via resonant ionization (detachment) of negative ions.

A closer inspection of data for the Al(1 1 1) and DLC target reveals a more narrow width and an onset at lower velocities of the resonance curve for the DLC surface (cf., Fig. 4). Such behaviour might indicate that instead of electron capture from the 3D-continuum of conduction band states, the 2D-continuum of the surface state for diamond surfaces will play a role in the formation of negative ions. Studies with metal targets with a projected band gap have shown that the surface state can have a pronounced effect on the formation of negative ions [26]. Preliminary calculations of the problem show that main features of the data shown in Figs. 3 and 4 can be reproduced by assuming electron capture and loss to the surface state continuum. On the other hand, similar negative ion fractions were observed with H-passivated DLC targets where signatures of the surface state disappear in photoelectron spectra [27]. Taking furthermore into account that the DLC target consists of poly-crystallites, studies with defined mono-crystalline diamond surfaces have to be performed, before definite conclusions in this respect can be drawn.

4. Conclusions

In this study we have scattered hydrogen and oxygen atoms as well as ions under a grazing angle of incidence from a DLC surface and have measured the charge fractions as function of projectile velocity. We observed that the negative charge fractions are independent of the projectile charge state, i.e., a charge state equilibrium is achieved during the scattering process. Key feature of our work is the finding of a type of kinematic resonance for the negative ion fractions. This resonance provides important information concerning the charge exchange interaction mechanisms and gives an upper limit for the application of DLC surfaces for negative ion conversion of fast ions. Our data show that for velocities above about 0.5 a.u., i.e., projectile energies of about 5 keV for hydrogen atoms and about 100 keV for oxygen atoms, the conversion is not efficient anymore and should be replaced by the detection of positive ions which dominate the charge state spectrum at higher energies. Whereas for hydrogen even at low energies the detection of positive ions appears as a good alternative, negative ion detection for oxygen is the clearly more favourable mode.

Acknowledgement

This work was supported by the Deutsche Forschungsgemeinschaft (DFG) under contract Wi 1336.

References

[1] J.A. Scheer, M. Wieser, P. Wurz, P. Bochsler, E. Hertzberg, S.A. Fuselier, F.A. Koeck, R.J. Nemanich, M. Schleberger, Adv. Space Res. 38 (2006) 664.
[2] D.J. McComas, F. Allegrini, P. Bochsler, M. Bzowski, E.R. Christian, G.B. Crew, R. DeMajistre, H. Fahr, H. Fichtner, P.C. Frisch, H.O. Funsten, S.A. Fuselier, G. Gloeckler, M. Gruntman, J. Heerikhuisen, V. Izmodenov, P. Hanzen, P. Knappenberger, S. Krimigis, H. Kucharek, M. Lee, G. Livadiotis, S. Livi, R.J. MacDowall, D. Mitchell, E. Möbius, T. Moore, N.V. Pogorelov, D. Reisenfeld, E. Roelof, L. Saul, N. Schwadron, P.W. Valek, R. Vnderspek, P. Wurz, G.P. Zank, Science 326 (2009) 959.
[3] P. Wurz, in: K. Scherer, H. Fichtner, E. Marsch (Eds.), The Outer Heliosphere: Beyond the Planets, Copernicus Gesellschaft e.V., Katlenburg-Lindau, Germany, 2000, p. 251.
[4] P. Wahlström, J. Scheer, P. Wurz, E. Hertzberg, S.A. Fuselier, J. Appl. Phys. 104 (2008) 034503.
[5] H.O. Funsten, F. Allegrini, G.B. Crew, R. DeMajistre, P.C. Frisch, S.A. Fuselier, M. Gruntmann, P. Janzen, D.J. Comas, E. Möbius, B. Randol, D.B. Reisenfeld, E.C. Roelof, N.A. Schwadron, Science 326 (2009) 964.
[6] P. Wurz, R. Schletti, M.R. Aellig, Surf. Sci. 373 (1997) 56.
[7] H. Winter, Prog. Surf. Sci. 63 (2000) 177.
[8] A.G. Borisov, D. Teillet-Billy, J.P. Gauyacq, Surf. Sci. 278 (1992) 99.
[9] J.N.M. van Wunnik, J.J.C. Geerlings, E.H.A. Graneman, J. Los, Surf. Sci. 131 (1983) 17.
[10] C.F.A. van Os, C. Lequijt, A.W. Kleyn, J. Los, Fusion Technol. 1 (1988) 598.
[11] U. von Gemmingen, R. Sizmann, Surf. Sci. 114 (1982) 445.
[12] A.W. Kleyn, in: A. Hershcovitch (Ed.), Production and Neutralization of Negative Ions and Beams, American Institute of Physics, New York, 1990, p. 3.
[13] J.P. Gauyacq, A.G. Borisov, J. Phys.: Condens. Matter 10 (1998) 6585.
[14] DLD40, Roentdek GmbH, Kelkheim, Ruppertshain, Germany.
[15] R. Pfandzelter, Phys. Rev. B 57 (1998) 15496.
[16] H. Winter, Phys. Rep. 367 (2002) 387.
[17] P. Wurz, J. Scheer, M. Wieser, J. Surf. Sci. Nanotech. 4 (2006) 394.
[18] J. Los, J.J.C. Geerlings, Phys. Rep. 190 (1990) 133.
[19] F. Wyputta, R. Zimny, H. Winter, Nucl. Instr. Meth. B 58 (1991) 379.
[20] C. Auth, A.G. Borisov, H. Winter, Phys. Rev. Lett. 75 (1995) 2292.
[21] A.G. Borisov, V. Sidis, H. Winter, Phys. Rev. Lett. 77 (1996) 1893.
[22] S. Ustaze, L. Guillemot, V. Esaulov, P. Nordlander, D.C. Lengreth, Surf. Sci. 415 (1998) L1027.
[23] P. Roncin, J. Villette, J.P. Atanas, H. Khemliche, Phys. Rev. Lett. 83 (1999) 864.
[24] H. Winter, C. Auth, A.G. Borisov, Nucl. Instr. Meth. B 115 (1996) 133.
[25] A. Mertens, H. Winter, Phys. Rev. Lett. 85 (2000) 2825.
[26] T. Hecht, H. Winter, A.G. Borisov, J.P. Gauyacq, A.K. Kazansky, Phys. Rev. Lett. 84 (2000) 2517.
[27] J. Ristein, R. Graupner, Adv. Solid State Phys. 36 (1997) 77.